

MTSI Algorithm for Frequencies Estimation of 2-D Superimposed Exponential Model in Multiplicative and Additive Noise which is Stationary

Jiawen Bian¹, Jing Xing^{2,3}, Huiming Peng¹ and Hongwei Li^{1,*}

¹ School of Mathematics and Physics, China University of Geosciences, Wuhan, 430074, China

² Institute of Statistics, Hubei University of Economics, Wuhan, 430205, China

³ Institute of Geophysics & Geomatics, China University of Geosciences, Wuhan, 430074, China

Received: 4 Aug. 2013, Revised: 6 Nov. 2013, Accepted: 7 Nov. 2013

Published online: 1 Jul. 2014

Abstract: In this paper, the frequencies estimation of two-dimensional (2-D) superimposed exponential model in zero-mean multiplicative and additive noise which is stationary, is considered by a computationally efficient statistics based iterative algorithm. The model we considered is a more general evanescent part of stationary random field as well as an important model in statistical signal processing and texture classifications. It is observed that the estimator is consistent and works quite well in terms of biases and mean squared errors. Moreover, the asymptotic distribution of the estimators for the frequencies is multivariate normal and the estimators attain the same convergence rate as the Least Squares Estimator (LSE) in additive noise. Finally, the effectiveness of the algorithm and the asymptotic results of the estimators for finite sample is verified via some numerical experiments.

Keywords: 2-D superimposed exponential model, modified three step iterative algorithm, Least squares estimator, convergence rate, random field.

1. Introduction

We consider the following 2-D superimposed exponential model in zero-mean stationary multiplicative and additive noise:

$$x(m, n) = \sum_{k=1}^p \beta_k(m, n) e^{i(u_k m + v_k n + \phi_k)} + \gamma(m, n), \quad (1)$$

where $\{x(m, n), m = 1, 2, \dots, M, n = 1, 2, \dots, N\}$ are observed values, $i = \sqrt{-1}$, $\{u_k, v_k\}$ is the unknown 2-D frequency pair and both of the frequencies lie in $[0, 2\pi)$. $\phi_k \in [0, 2\pi)$ is the unknown phase. Multiplicative noise $\{\beta_k(m, n)\}$ and additive noise $\{\gamma(m, n)\}$ are both stationary real random variables as follows:

$$\beta_k(m, n) = \sum_{s=-\infty}^{+\infty} \sum_{l=-\infty}^{+\infty} a_k(s, l) \varepsilon_k(m-s, n-l), \quad (2)$$

$$\gamma(m, n) = \sum_{s=-\infty}^{+\infty} \sum_{l=-\infty}^{+\infty} a_0(s, l) \varepsilon_0(m-s, n-l), \quad (3)$$

where the driving processes $\{\varepsilon_k(m, n) (k = 0, 1, \dots, p)\}$ are all independent identically distribution (i.i.d.) random variables with mean zero and variance σ_k^2 . The coefficients $\{a_k(s, l) (k = 0, 1, \dots, p)\}$ are all absolutely summable i.e.

$$\sum_{s=-\infty}^{+\infty} \sum_{l=-\infty}^{+\infty} |a_k(s, l)| < +\infty. \quad (4)$$

In this paper, we concentrate on the estimation of the frequencies (u_k, v_k) , given a sample of size M and N , namely $x(1, 1), \dots, x(M, N)$. The number of components p is assumed to be known in advance. We make the following assumptions:

- (i) The driving process of multiplicative and additive noise i.e. $\{\varepsilon_k(m, n) (k > 0)\}$ and $\{\varepsilon_0(m, n)\}$ have finite fourth order moment and they are independent with each other;
- (ii) The frequency pairs satisfy: $(u_j, v_j) \neq (u_k, v_k), (u_j, v_j) \neq 2(u_k, v_k), (u_k + u_l, v_k + v_l) \neq (2u_j, 2v_j)$ for different

* Corresponding author e-mail: hwli@cug.edu.cn

$k, j, l;$

$$(iii) 0 < \limsup_{\min\{M,N\} \rightarrow +\infty} M/N < +\infty.$$

It can be seen from assumption (i) that the multiplicative noise and additive noise are independent. It is also noted that the assumption (ii) is some critical, however, it can be relaxed (see Remark 1). If assumption (ii) is not satisfied, the proposed algorithm is still feasible, but the asymptotic distribution of the estimator for frequencies will be changed accordingly.

Estimation of 2-D frequencies from a finite subset of data in noise is an important problem in many practical applications, such as joint frequency-angle estimation, 2-D spectral estimation, geophysics, radar imaging and texture classifications [1,2]. In practical the noise tends to be color [3,4] which make the estimation for the parameter to be more difficult. The parameter estimation of 2-D superimposed exponential model in zero-mean multiplicative and additive noise is a special case of the general problem of estimating the parameters of a complex-valued homogeneous random field with mixed spectral distribution from a single observed realization of it [5,6]. According to the Wold decomposition theory of [7], any 2-D regular and homogeneous discrete random field can be represented as a sum of two mutually orthogonal components: a purely indeterministic field and a deterministic one. The deterministic component is further orthogonally decomposed into a harmonic field and a countable number of mutually orthogonal evanescent fields. The purely indeterministic component has a unique white innovations driven moving-average representation which is stationary as the second term of model (1) we considered, where the evanescent component is a special case of the first term of model (1) although the autoregressive (AR) process [5] considered can be non-stationary.

It can be seen that model (1) is a non-stationary model and the parameter estimation for non-stationary model is a harder problem than for stationary model [8]. Much work focus on the parameters estimation of homogeneous random field consisting of harmonic field and purely indeterministic field i.e. harmonic or superimposed exponential model in additive noise [9,10,11,12,13] while little attention has been paid to estimate the parameters of homogeneous random field consisting of evanescent field and purely indeterministic field. [5] used a two-stage procedure to jointly estimate the parameters of the harmonic, evanescent components of a real-valued homogeneous random field. At the first stage, a suboptimal initial estimate for the parameters of the spectral support of the evanescent and harmonic components is obtained by solving a set of overdetermined 2-D normal equations of a high-order linear predictor of the observed data. Then the initial estimators were refined by iterative maximization of the conditional likelihood of the observed data. Although a separable LSE procedure was utilized in the second stage,

however, there are so many parameters to be estimated simultaneously that the computation is complex and the precision is limited. It is necessary to find a more accurate and computationally efficient algorithm for the estimation of the frequencies of the evanescent component. It is known that both maximum likelihood estimator (MLE) [14] and LSE [9,10,15] have excellent statistical performance when there exists only harmonic and purely indeterministic component in the random field, and MLE is equivalent to LSE when there is only additive Gaussian noise. The orders of convergence rate of the LSE for $\{u_k\}$ and $\{v_k\}$ are $O_p(M^{-3/2}N^{-1/2})$ and $O_p(M^{-1/2}N^{-3/2})$ respectively (here $O_p(\cdot)$ means bo-unded in probability), which are expected to be the best [10]. But their high computation burden limits their applications in practice. Therefore, some sub-optimal approaches with less amount of computation and some degradation in performance, were studied extensively, such as the subspace-based methods (e.g. 2-D ESPRIT-type method [13], MEMP method [16], 2-D Prony method [17] and ACMP method [18]).

However, the optimal choice is to find a computationally efficient LSE equivalent algorithm for this purpose. Recently, [12] generalized the seven step iterative (SSI) algorithm [19] and three step iterative (TSI) algorithm [20,21,22] to estimate the parameters of 2-D harmonic in additive noise. It was observed that both SSI and TSI estimators for the frequencies of 1-D harmonics attain the same convergence rate as LSE and have an asymptotic normal distribution while TSI is more computationally efficient than SSI. It must be pointed out that [20,21] considered the parameter estimation of 1-D harmonic with nonzero mean amplitude, in additive noise and multiplicative noise respectively. [22] considered the parameter estimation of 1-D harmonic with zero mean multiplicative and additive noise. The three estimators above laid a good basis for the TSI estimation of parameters of 2-D harmonic, which is the deterministic part of a 2-D regular and homogeneous random field. Most recently, [23] further developed the TSI algorithm to estimate the frequencies of random field consisting of evanescent and purely indeterministic component which are both constituted of i.i.d. random processes. It is observed that the estimators are consistent and attain the same convergence rate as LSE. However, the evanescent and purely indeterministic component are more widely to be described as stationary processes [5,25]. So it is necessary to consider the parameters estimation when the evanescent and purely indeterministic component are constituted of stationary random processes.

But no where, at least not known to the authors, the TSI estimator has been considered for the frequencies of random field consisting of evanescent and purely indeterministic component which are both constituted of stationary random processes. Stimulated by the work of [5], [12] and [23], in this paper, we use a modified TSI (MTSI) algorithm which is based on a two-stage

procedure to estimate the frequencies of harmonics in zero-mean stationary multiplicative and additive noise, as well as examine the efficiency of the MTSI algorithm for model (1) and study the asymptotic behaviors for the MTSI estimators of frequencies. It is important to be observed that the TSI algorithm in [12] considered the frequencies estimation of harmonic and purely indeterministic component and can not be used directly for the frequency estimation of evanescent and purely indeterministic component under zero mean multiplicative and additive noise. It is also noticed that although [23] also generalized the TSI algorithm to estimate the frequencies of evanescent and purely indeterministic component under zero-mean multiplicative and additive noise condition, however, the evanescent and purely indeterministic component are considered as i.i.d. random processes which are not suitable for the more general stationary processes. Moreover, although the squaring of the observed values in [23] can make the initial estimator and the iterative process feasible, the stationary property of the evanescent and purely indeterministic component seems to decrease the performance of the TSI algorithm severely, thus makes the consistency and asymptotic normality property for the TSI estimators of frequencies in our considered model not immediate in this case. The estimation procedure in this paper is divided into two stages. At the first stage, we use the half value of 2-D periodogram maximizers over Fourier frequencies as the initial estimators. At the second stage, a statistics based three iterative process is utilized to refine the initial estimators. It is observed that if the initial estimators are accurate up to the order $O_p(M^{-1})$ and $O_p(N^{-1})$ for the frequencies u_j and v_j respectively, then the MTSI algorithm produces fully efficient estimators of frequencies with convergence rate of $O_p(M^{-3/2}N^{-1/2})$ and $O_p(M^{-1/2}N^{-3/2})$ for u_j and v_j respectively, which are the convergence rate of the LSE's [9] in additive noise. Since the MTSI algorithm needs only three steps to converge. So it is computationally efficient and can be served as online implementation.

The rest of the paper is organized as follows. In Section 2, we give the initial estimators of frequencies based on the 2-D periodogram. The proposed algorithm and the asymptotic distribution of the estimator is presented in Section 3. In Section 4, we present some numerical experiments to observe the efficiency of the algorithm. Finally, we conclude the paper in Section 5. All the proofs are provided in the Appendix.

2. Initial estimator

We use the 2-D periodogram maximizers at the Fourier frequencies as the initial estimator, which is defined as

follows:

$$f(u, v) = \frac{1}{MN} \left| \sum_{m=1}^M \sum_{n=1}^N x^2(m, n) e^{-i(mu+nv)} \right|. \quad (5)$$

Although Fourier transformation is efficient for the frequency estimation of stationary signal [24]. It can be observed that Fourier transform can also be used for the initial frequency estimator of non-stationary signal [23], especially for the non-zero mean exponential signal model [21]. Since $\{\beta_k(m, n)\}$ and $\{\gamma(m, n)\}$ in model (1) are both i.i.d. zero-mean random processes and the square of the observed values in model (1) can be seen as complex harmonics with non-zero mean amplitude and twice of the original frequencies and phases, so the estimation of frequencies can also be obtained by squaring the observed values. In practice, we employ the 2-D FFT of $x^2(m, n)$ to find the p local maxima of $f(u, v)$ and take the half values of them as the initial estimates. It is observed that [12] also used a periodogram based initial estimator. Different from (5), [12] used an average estimator of the 1-D periodogram maximizers of each column of the 2-D observed values while we use the 2-D periodogram maximizers as the initial estimator.

It is known that the 2-D periodogram maximizers over Fourier frequencies do not generally provide the accuracy of the estimators up to the order $O_p(M^{-1})$ and $O_p(N^{-1})$ for the frequencies u_j and v_j respectively. To overcome this problem, we employ a varying sample size technique as in [12] in the following estimation, i.e. increasing the sample size gradually with the increase of steps.

3. MTSI estimator

In this section, a MTSI algorithm similar with that in [23] are proposed to increase the accuracy of the frequencies in zero-mean stationary multiplicative and additive noise. Then the asymptotic behavior of the MTSI estimator of frequencies under this condition is analyzed. For convenience, in the following we note $\mathbf{u} = (u_1, \dots, u_p)$, $\mathbf{v} = (v_1, \dots, v_p)$, $\tilde{\mathbf{u}} = (\tilde{u}_1, \dots, \tilde{u}_p)$, $\tilde{\mathbf{v}} = (\tilde{v}_1, \dots, \tilde{v}_p)$, $\hat{\mathbf{u}} = (\hat{u}_1, \dots, \hat{u}_p)$ and $\hat{\mathbf{v}} = (\hat{v}_1, \dots, \hat{v}_p)$ as the vectors of the frequency pairs to be estimated, the vectors of frequency pairs before iteration and the vectors of frequency pairs after iteration respectively. Given a consistent estimator $\tilde{\mathbf{u}}$ and $\tilde{\mathbf{v}}$ of model (1), we compute $\hat{\mathbf{u}}$ and $\hat{\mathbf{v}}$ as follows:

$$\begin{aligned} \hat{\mathbf{u}} &= \tilde{\mathbf{u}} + \frac{6}{M^2} \text{Im}[\mathbf{A}_{M,N} \odot \mathbf{C}_{M,N}], \\ \hat{\mathbf{v}} &= \tilde{\mathbf{v}} + \frac{6}{N^2} \text{Im}[\mathbf{B}_{M,N} \odot \mathbf{C}_{M,N}], \end{aligned} \quad (6)$$

where $\text{Im}[\cdot]$ denotes the imaginary part of a complex number and \odot denotes Hadamard product [26]. $\mathbf{A}_{M,N}$, $\mathbf{B}_{M,N}$ and $\mathbf{C}_{M,N}$ are vectors with length p and the j -th

elements of $\mathbf{A}_{M,N}$, $\mathbf{B}_{M,N}$ and $\mathbf{C}_{M,N}$ are as follows:

$$\mathbf{A}_{M,N}(j) = \sum_{m=1}^M \sum_{n=1}^N x^2(m,n) \left(m - \frac{M}{2}\right) e^{-2i(\tilde{u}_j m + \tilde{v}_j n)}, \tag{7}$$

$$\mathbf{B}_{M,N}(j) = \sum_{m=1}^M \sum_{n=1}^N x^2(m,n) \left(n - \frac{N}{2}\right) e^{-2i(\tilde{u}_j m + \tilde{v}_j n)}, \tag{8}$$

$$\mathbf{C}_{M,N}(j) = 1 \left/ \sum_{m=1}^M \sum_{n=1}^N x^2(m,n) e^{-2i(\tilde{u}_j m + \tilde{v}_j n)} \right. . \tag{9}$$

The precision can be improved by (6) step by step from any consistent initial estimator $\tilde{\mathbf{u}}$ and $\tilde{\mathbf{v}}$. The asymptotic distribution and the convergence rate for the estimators of frequencies after three iterations i.e. $\hat{\mathbf{u}}$ and $\hat{\mathbf{v}}$ are provided in the following theorem:

Theorem 1. If $\tilde{\mathbf{u}} - \mathbf{u} = O_p(M^{-1-\delta})\mathbf{I}_p$ and $\tilde{\mathbf{v}} - \mathbf{v} = O_p(N^{-1-\delta})\mathbf{I}_p$, where $\delta \in (0, 1]$, then

(a) $\hat{\mathbf{u}} - \mathbf{u} = O_p(M^{-1-2\delta})\mathbf{I}_p$, $\hat{\mathbf{v}} - \mathbf{v} = O_p(N^{-1-2\delta})\mathbf{I}_p$, for $0 < \delta < \frac{1}{2}$,

(b) $\left[M^{\frac{3}{2}} N^{\frac{1}{2}} (\hat{\mathbf{u}} - \mathbf{u}), M^{\frac{1}{2}} N^{\frac{3}{2}} (\hat{\mathbf{v}} - \mathbf{v}) \right] \xrightarrow{\mathcal{L}} \mathcal{N}_{2p} \left(\mathbf{0}, \begin{bmatrix} \Sigma_1 & \mathbf{0} \\ \mathbf{0} & \Sigma_2 \end{bmatrix} \right)$, for $\frac{1}{2} \leq \delta \leq 1$,

where

$$\Sigma_2 = \Sigma_1, (\Sigma_1)_{jj} = \frac{E_j}{F_j},$$

for $j=1, 2, \dots, p$ and

$$(\Sigma_1)_{j\tau} = \frac{G_{j\tau}}{H_{j\tau}},$$

for $j \neq \tau$. \mathbf{I}_p denotes a p -order vector with its all elements to be 1. \mathcal{L} denotes convergence in distribution.

Proof. See Appendix.

Remark. It can be seen from the Appendix that if the assumption(ii) is not satisfied, the MTSI algorithm will be still efficient. But the diagonal term in Σ_1 will change, i.e. if $(u_\tau, v_\tau) = 2(u_j, v_j)$ then the seventh term in $(\Sigma_1)_{jj}$ will be changed to:

$$\left\{ 4 \left| \sum_{s=-\infty}^{+\infty} \sum_{l=-\infty}^{+\infty} \sum_{s'=-\infty}^{+\infty} \sum_{l'=-\infty}^{+\infty} a_\tau(s,l) a_0(s',l') \right|^2 \right. \\ \times \sigma_0^2 \sin^2(\phi_\tau - 2\phi_j) + 4 \sum_{k \neq \tau} \left| \sum_{s=-\infty}^{+\infty} \sum_{l=-\infty}^{+\infty} \sum_{s'=-\infty}^{+\infty} \sum_{l'=-\infty}^{+\infty} \right. \\ \left. a_k(s,l) a_0(s',l') e^{i \left[\frac{(u_k - 2u_j)}{2} (s+s') + \frac{(v_k - 2v_j)}{2} (l+l') \right]} \right|^2 \sigma_0^2 \sigma_k^2 \left. \right\} \\ \left/ \left[\sum_{s=-\infty}^{+\infty} \sum_{l=-\infty}^{+\infty} a_j^2(s,l) \right]^2 \right. \sigma_j^4,$$

and if $(u_\tau + u_\gamma, v_\tau + v_\gamma) = (2u_j, 2v_j)$ then the last term in $(\Sigma_1)_{jj}$ will be changed to:

$$\left\{ 4 \sum_{k \neq \tau} \sum_{l < k, l \neq \gamma} \left| \sum_{s=-\infty}^{+\infty} \sum_{t=-\infty}^{+\infty} \sum_{s'=-\infty}^{+\infty} \sum_{t'=-\infty}^{+\infty} a_k(s,t) a_l(s',t') \right. \right. \\ \left. \left. e^{i \left[\frac{(u_k + u_l - 2u_j)}{2} (s+s') + \frac{(v_k + v_l - 2v_j)}{2} (t+t') \right]} \right|^2 \sigma_k^2 \sigma_l^2 \right. \\ \left. + 4 \left| \sum_{s=-\infty}^{+\infty} \sum_{t=-\infty}^{+\infty} \sum_{s'=-\infty}^{+\infty} \sum_{t'=-\infty}^{+\infty} a_\tau(s,t) a_\gamma(s',t') \right|^2 \sigma_\tau^2 \sigma_\gamma^2 \right. \\ \left. \times \sin^2(\phi_\tau + \phi_\gamma - 2\phi_j) \right\} \\ \left/ \left[\sum_{s=-\infty}^{+\infty} \sum_{l=-\infty}^{+\infty} a_j^2(s,l) \right]^2 \right. \sigma_j^4.$$

The detailed procedure of the two-stage algorithm is described as the following. We start with the initial estimates of the 2-D periodogram maximizers and improve it step by step by the recursive process above. The m -th step estimators $\hat{\mathbf{u}}^{(m)}$ and $\hat{\mathbf{v}}^{(m)}$ ($m = 1, 2, 3$) are computed from the $(m - 1)$ -th step estimators $\hat{\mathbf{u}}^{(m-1)}$ and $\hat{\mathbf{v}}^{(m-1)}$ respectively by the formulas as follows:

$$\hat{\mathbf{u}}^{(m)} = \hat{\mathbf{u}}^{(m-1)} + \frac{6}{M_m^2} \text{Im} [\mathbf{A}_{M_m, N_m} \odot \mathbf{C}_{M_m, N_m}], \\ \hat{\mathbf{v}}^{(m)} = \hat{\mathbf{v}}^{(m-1)} + \frac{6}{N_m^2} \text{Im} [\mathbf{B}_{M_m, N_m} \odot \mathbf{C}_{M_m, N_m}], \tag{10}$$

where $\hat{\mathbf{u}}^m = (\hat{u}_1^m, \dots, \hat{u}_p^m)$ and $\hat{\mathbf{v}}^m = (\hat{v}_1^m, \dots, \hat{v}_p^m)$ are the estimators after the m -th iteration, $\mathbf{A}_{M_m, N_m}(j)$, $\mathbf{B}_{M_m, N_m}(j)$ and $\mathbf{C}_{M_m, N_m}(j)$ can be obtained from (7)-(9) by replacing M, N, \tilde{u}_j and \tilde{v}_j with $M_m, N_m, \hat{u}_j^{(m-1)}$ and $\hat{v}_j^{(m-1)}$ respectively. The detailed three-step iteration process is as follows:

Step 1 With $m = 1$, choose $M_1 = M^{0.8}$, $N_1 = N^{0.8}$, $\hat{\mathbf{u}}^{(0)} = \tilde{\mathbf{u}}$ and $\hat{\mathbf{v}}^{(0)} = \tilde{\mathbf{v}}$, which are the initial estimates obtained by the 2-D periodogram maximizer.

Note that $\tilde{\mathbf{u}} - \mathbf{u} = O_p(M^{-1})\mathbf{I}_p = O_p(M_1^{-1-\frac{1}{4}})\mathbf{I}_p$ and $\tilde{\mathbf{v}} - \mathbf{v} = O_p(N^{-1})\mathbf{I}_p = O_p(N_1^{-1-\frac{1}{4}})\mathbf{I}_p$. Taking $M_1 = M^{0.8}$, $N_1 = N^{0.8}$, $\hat{\mathbf{u}}^{(0)} = \tilde{\mathbf{u}}$ and $\hat{\mathbf{v}}^{(0)} = \tilde{\mathbf{v}}$ in (10), and applying part (a) of Theorem 1, we obtain

$$\hat{\mathbf{u}}^{(1)} - \mathbf{u} = O_p(M_1^{-1-\frac{1}{2}})\mathbf{I}_p = O_p(M^{-\frac{6}{5}})\mathbf{I}_p, \\ \hat{\mathbf{v}}^{(1)} - \mathbf{v} = O_p(N_1^{-1-\frac{1}{2}})\mathbf{I}_p = O_p(N^{-\frac{6}{5}})\mathbf{I}_p.$$

Step 2 With $m = 2$, choose $M_2 = M^{0.9}$ and $N_2 = N^{0.9}$, compute $\hat{\mathbf{u}}^{(2)}$ and $\hat{\mathbf{v}}^{(2)}$ from $\hat{\mathbf{u}}^{(1)}$ and $\hat{\mathbf{v}}^{(1)}$. Since $\hat{\mathbf{u}}^{(1)} - \mathbf{u} = O_p(M^{-\frac{6}{5}})\mathbf{I}_p = O_p(M_2^{-1-\frac{1}{3}})\mathbf{I}_p$ and $\hat{\mathbf{v}}^{(1)} - \mathbf{v} = O_p(N^{-\frac{6}{5}})\mathbf{I}_p = O_p(N_2^{-1-\frac{1}{3}})\mathbf{I}_p$, use part (a) of Theorem 1 again, we have

$$\hat{\mathbf{u}}^{(2)} - \mathbf{u} = O_p(M_2^{-1-\frac{2}{3}})\mathbf{I}_p = O_p(M^{-\frac{3}{2}})\mathbf{I}_p, \\ \hat{\mathbf{v}}^{(2)} - \mathbf{v} = O_p(N_2^{-1-\frac{2}{3}})\mathbf{I}_p = O_p(N^{-\frac{3}{2}})\mathbf{I}_p.$$

$$\begin{aligned}
 E_j &= \frac{3}{2} \left\{ \sum_{k \neq j} \left| \sum_{s=-\infty}^{+\infty} \sum_{l=-\infty}^{+\infty} a_k^2(s, l) e^{2i[(u_k - u_j)s + (v_k - v_j)l]} \right|^2 \left[E(\epsilon_k^4) - \sigma_k^4 \right] \right. \\
 &+ 4 \sum_{k \neq j} \left| \sum_{s=-\infty}^{+\infty} \sum_{l=-\infty}^{+\infty} \sum_{s' \neq s} \sum_{l' \neq l} a_k(s, l) a_k(s', l') e^{i[(u_k - u_j)(s+s') + (v_k - v_j)(l+l')]} \right|^2 \sigma_k^4 \\
 &+ 4 \sum_{k \neq j} \left| \sum_{s=-\infty}^{+\infty} \sum_{l=-\infty}^{+\infty} \sum_{l' \neq l} a_k(s, l) a_k(s, l') e^{i[2s(u_k - u_j) + (v_k - v_j)(l+l')]} \right|^2 \sigma_k^4 + \left| \sum_{s=-\infty}^{+\infty} \sum_{l=-\infty}^{+\infty} a_0^2(s, l) e^{2i(u_j s + v_j l)} \right|^2 \left[E(\epsilon_0^4) - \sigma_0^4 \right] \\
 &+ 4 \left| \sum_{s=-\infty}^{+\infty} \sum_{l=-\infty}^{+\infty} \sum_{s' \neq s} \sum_{l' \neq l} a_0(s, l) a_0(s', l') e^{i[u_j(s+s') + v_j(l+l')]} \right|^2 \sigma_0^4 + 4 \left| \sum_{s=-\infty}^{+\infty} \sum_{l=-\infty}^{+\infty} \sum_{l' \neq l} a_0(s, l) a_0(s, l') e^{i[2su_j + v_j(l+l')]} \right|^2 \sigma_0^4 \\
 &+ 4 \sum_{k=1}^p \left| \sum_{s=-\infty}^{+\infty} \sum_{l=-\infty}^{+\infty} \sum_{s' \neq s} \sum_{l' \neq l} a_k(s, l) a_0(s', l') e^{i\left[\frac{(u_k - 2u_j)}{2}(s+s') + \frac{(v_k - 2v_j)}{2}(l+l')\right]} \right|^2 \sigma_0^2 \sigma_k^2 \\
 &+ 4 \sum_{k=1}^p \sum_{l=1}^p \left| \sum_{s=-\infty}^{+\infty} \sum_{t=-\infty}^{+\infty} \sum_{s' \neq s} \sum_{t' \neq t} a_k(s, t) a_l(s', t') e^{i\left[\frac{(u_k + u_l - 2u_j)}{2}(s+s') + \frac{(v_k + v_l - 2v_j)}{2}(t+t')\right]} \right|^2 \sigma_k^2 \sigma_l^2 \left. \right\}, \\
 F_j &= \left[\sum_{s=-\infty}^{+\infty} \sum_{l=-\infty}^{+\infty} a_j^2(s, l) \right]^2 \sigma_j^4, H_{j\tau} = \left[\sum_{s=-\infty}^{+\infty} \sum_{l=-\infty}^{+\infty} a_j^2(s, l) \right] \left[\sum_{s=-\infty}^{+\infty} \sum_{l=-\infty}^{+\infty} a_\tau^2(s, l) \right], \\
 G_{j\tau} &= -6 \left| \sum_{s=-\infty}^{+\infty} \sum_{t=-\infty}^{+\infty} \sum_{s' \neq s} \sum_{t' \neq t} a_j(s, t) a_\tau(s', t') e^{i\left[\frac{(u_j - u_\tau)}{2}(s+s') + \frac{(v_j - v_\tau)}{2}(t+t')\right]} \right|^2,
 \end{aligned}$$

Step 3 With $m = 3$, choose $M_3 = M$ and $N_3 = N$, compute $\hat{\mathbf{u}}^{(3)}$ and $\hat{\mathbf{v}}^{(3)}$ from $\hat{\mathbf{u}}^{(2)}$ and $\hat{\mathbf{v}}^{(2)}$, apply part (b) of Theorem 1, we have

$$(M^{\frac{3}{2}} N^{\frac{1}{2}} (\hat{\mathbf{u}} - \mathbf{u}), M^{\frac{1}{2}} N^{\frac{3}{2}} (\hat{\mathbf{v}} - \mathbf{v})) \xrightarrow{\mathcal{L}} \mathcal{N}_{2p} \left(\mathbf{0}, \begin{bmatrix} \Sigma_1 & \mathbf{0} \\ \mathbf{0} & \Sigma_2 \end{bmatrix} \right).$$

Table 1: The average estimates of the Initial and MTSI estimator based on 100 replications, as well as the corresponding SEs and ASEs of the two frequency pairs when $M=N=128$

σ_0	ESTI	Fr11	Fr12	Fr21	Fr22
0.5	PARA	0.50000	1.50000	0.60000	1.60000
	INIT	0.49087	1.52171	0.58905	1.59534
	MTSI	0.50009	1.50002	0.59999	1.60001
	SE	2.334e-4	2.2215e-4	1.584e-4	1.651e-4
	ASE	2.179e-4	2.1797e-4	1.555e-4	1.555e-4
1	PARA	0.50000	1.50000	0.60000	1.60000
	INIT	0.49087	1.52170	0.58904	1.59534
	MTSI	0.49999	1.50001	0.59997	1.60003
	SE	2.826e-4	2.9262e-4	2.010e-4	2.124e-4
	ASE	2.720e-4	2.7200e-4	1.976e-4	1.976e-4
1.5	PARA	0.50000	1.50000	0.60000	1.60000
	INIT	0.49087	1.52170	0.58904	1.59534
	MTSI	0.49994	1.50002	0.59999	1.60003
	SE	4.633e-4	4.3237e-4	2.584e-4	2.726e-4
	ASE	3.503e-4	3.5039e-4	2.590e-4	2.590e-4

It can be seen that a similar three-step iterative process is used in [12]. The difference lies in that we use the varying sample on M and N simultaneously while [12] just use the varying sample on M or N solely. Moreover, the factor of the iterative term in this paper is different with that in [12] so as to deal with the estimation of zero-mean multiplicative noise condition. It is observed that if at any step, the estimators are accurate up to the order $O_p(M^{-1-\delta})$ and $O_p(N^{-1-\delta})$ for u_j and $v_j (j = 1, \dots, p)$ respectively, the method provides estimators with orders being improved to $O_p(M^{-1-2\delta})$ and $O_p(N^{-1-2\delta})$ respectively for $0 < \delta < \frac{1}{2}$ and if $\frac{1}{2} \leq \delta \leq 1$, then it provides the efficient estimators with convergence rate of $O_p(M^{-3/2} N^{-1/2})$ and $O_p(M^{-1/2} N^{-3/2})$ for the frequency pairs. Comparing with [23], it is observed that the MTSI algorithm still works well and the MTSI estimators for the frequency pairs have the same convergence rate as that of the i.i.d. noise condition.

Remark. There are several other exponents we used above can be chosen so that the iterative process will converge in three steps. In another word, they are not unique. For example another set of choices can be $M_1 = M^{0.75}$, $N_1 = N^{0.75}$; $M_2 = M^{0.85}$, $N_2 = N^{0.85}$ and $M_3 = M$, $N_3 = N$. It is not possible to choose a set of exponents to make the iterative process converge in less than three steps, but it is sure for several sets of exponents to take more than three steps to converge. It is also noted that we

take the same set of exponents for the first and second dimension. Actually, they can be different provided that they can guarantee MTSI to converge in three steps.

4. Numerical experiment

In this section we present some numerical results to observe how the proposed algorithm works and the asymptotic results behave for finite sample sizes. We consider the following model:

$$x(m,n) = \beta_1(m,n)e^{i(0.5m+1.5n+\pi/4)} + \beta_2(m,n)e^{i(0.6m+1.6n+\pi/3)} + \gamma(m,n), \quad (11)$$

where multiplicative noise $\{\beta_1(m,n)\}$, $\{\beta_2(m,n)\}$ and additive noise $\{\gamma(m,n)\}$ are all MA processes whose driving processes are $\{\varepsilon_1(m,n)\}$, $\{\varepsilon_2(m,n)\}$ and $\{\varepsilon_0(m,n)\}$ respectively, which are all i.i.d. Gaussian random variables with mean zero and variance 2, 3 and σ_0^2 respectively. The structure of $\{\beta_1(m,n)\}$, $\{\beta_2(m,n)\}$ and $\{\gamma(m,n)\}$ are as follows

$$\begin{aligned} \beta_1(m,n) &= \varepsilon_1(m,n) + 0.6\varepsilon_1(m-1,n-1), \\ \beta_2(m,n) &= \varepsilon_2(m,n) - 0.4\varepsilon_2(m-1,n-1), \\ \gamma(m,n) &= \varepsilon_0(m,n) + 0.5\varepsilon_0(m-1,n-1). \end{aligned}$$

Although the existing of the additive and multiplicative noise both decrease the performance of the estimation, however, the multiplicative noise is also useful for estimating the frequencies observed from Section 2 and the proof of Theorem 1. To assess the sensitivity of the model to different noise levels, we fix the multiplicative noise level and plot three different additive noise level namely $\sigma_0 = 0.5, 1$ and 1.5 . To present the consistency, we take the sample sizes as $M=N=128, 256$ and 512 . We also take $M=512, N=128$ to examine the performance when M is not equal to N .

For illustration purpose for the efficiency of the initial estimator, we plot the 2-D periodogram function of the original observations in Figure 1-Figure 4 for sample size (a) $M=N=128$, (b) $M=N=256$, (c) $M=N=512$ and (d) $M=512, N=128$ respectively. For comparison purpose, we also plot the 2-D periodogram function of the squared values of the original observations in Figure 5-Figure 8 for the considered model corresponding to the above sample size (a)-(d) respectively. The standard deviation of the additive noise is taken as 1.5 for all the cases. Comparing the corresponding Figure 1-Figure 4 with Figure 5-Figure 8 for the same sample size, it is obvious that there is no peak in the plot of the periodogram of the original observations at the real frequency pairs while the squaring of the original observations makes the peaks obvious at the frequency pairs to be estimated. It is because the spectra of the observations has the same magnitude at all the frequency pairs when the multiplicative noise is zero-mean. However, the squaring of the observations makes the magnitude much larger at the frequency pairs to be estimated than at the other

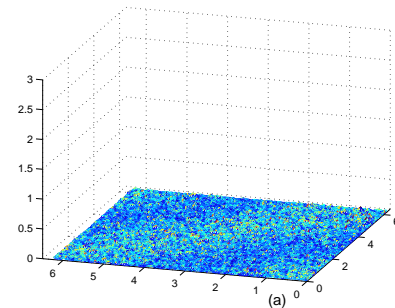


Figure 1: Plot of the 2-D periodogram function of the original observations for model (11) when (a) $M=N=128$ with $\sigma_0=1.5$

frequency pairs. It is known that the number of peaks in the periodogram function plot roughly gives an estimate of the number of frequencies. It depends on the magnitude of the amplitude associated with each effective frequency and the noise level. From Figure 5-Figure 8, it is quite clear that there are three peaks which include the one at $(0,0)$ for Figure 5-Figure 8. Actually, $(0,0)$ is a false frequency pair as the additive noise is real, thus cause the periodogram maximizer of the squared observations at $(0,0)$. The remained two peaks are the plot of the two pairs of frequencies to be estimated actually.

Table 2: The average estimates of the Initial and MTSI estimator based on 100 replications, as well as the corresponding SEs and ASEs of the two frequency pairs when $M=N=256$

σ_0	EST	Fr11	Fr12	Fr21	Fr22
0.5	PARA	0.50000	1.50000	0.60000	1.60000
	INIT	0.50314	1.49716	0.60132	1.59534
	MTSI	0.49999	1.49998	0.60000	1.60000
	SE	5.446e-5	5.736e-5	4.213e-5	3.939e-5
	ASE	5.449e-5	5.449e-5	3.889e-5	3.889e-5
1	PARA	0.50000	1.50000	0.60000	1.60000
	INIT	0.50314	1.49716	0.60132	1.59534
	MTSI	0.50000	1.50002	0.59999	1.59999
	SE	6.828e-5	7.476e-5	5.094e-5	4.947e-5
	ASE	6.800e-5	6.800e-5	4.941e-5	4.941e-5
1.5	PARA	0.50000	1.50000	0.60000	1.60000
	INIT	0.50314	1.49716	0.60132	1.59534
	MTSI	0.50002	1.49999	0.59999	1.60002
	SE	8.779e-5	8.913e-5	6.438e-5	6.506e-5
	ASE	8.759e-5	8.759e-5	6.476e-5	6.476e-5

Now for each sample size, we estimate the frequencies based on the MTSI algorithm. In all cases we consider the periodogram maximizer at the Fourier frequencies as the initial estimator. We report the average estimates of the two pairs of frequencies (Fr11, Fr12), (Fr21, Fr22) and the standard errors (SEs) over 100 replications. For comparison purpose, we also report the initial estimates

as well as the true values of frequencies and the corresponding asymptotic standard errors (ASEs). All the estimators (ESTI) are reported in Tables 1-4 for the average estimates and standard deviations of frequencies of model (11) corresponding to $M=N=128, 256, 512$ and $M=512, N=128$ respectively, in Table 5 for the covariances of Fr11 and Fr21, and in Table 6 for the covariances of Fr12 and Fr22 when $M=N=128, 256, 512$ and $M=512, N=128$ respectively. In Tables 1-4 and for each σ_0 , the first row represents the true parameter values (PARA) and the initial estimates are reported at the second row (INIT), the third row represents the MTSI estimates and the SEs of the MTSI estimates are reported at the fourth row. Finally, we reported the ASEs at the last row. In Tables 5-6 and for each σ_0 , the first row represents the covariances (COVs) for the estimates of corresponding frequencies between different frequency pairs, and the asymptotic covariances (ACOVs) for the estimates of corresponding frequencies between different frequency pairs are reported at the second row.

Table 3: The average estimates of the Initial and MTSI estimator based on 100 replications, as well as the corresponding SEs and ASEs of the two frequency pairs when $M=N=512$

σ_0	ESTI	Fr11	Fr12	Fr21	Fr22
0.5	PARA	0.50000	1.50000	0.60000	1.60000
	INIT	0.49701	1.49716	0.60132	1.60147
	MTSI	0.50000	1.49999	0.59999	1.60000
	SE	1.388e-5	1.495e-5	9.737e-6	1.011e-5
	ASE	1.362e-5	1.362e-5	9.713e-6	9.713e-6
1	PARA	0.50000	1.50000	0.60000	1.60000
	INIT	0.49701	1.49716	0.60132	1.60147
	MTSI	0.50000	1.50000	0.59999	1.59999
	SE	1.698e-5	1.715e-5	1.240e-5	1.326e-5
	ASE	1.700e-5	1.700e-5	1.235e-5	1.235e-5
1.5	PARA	0.50000	1.50000	0.60000	1.60000
	INIT	0.49701	1.49716	0.60132	1.60147
	MTSI	0.50000	1.50000	0.59999	1.59999
	SE	2.232e-5	2.254e-5	1.660e-5	1.625e-5
	ASE	2.189e-5	2.189e-5	1.619e-5	1.619e-5

The following observations are very clear from the numerical experiments. It is observed from Tables 1-4 that the MTSI estimates are very close to the true parameter values and are better than the initial estimates in nearly all the cases considered. It is immediate that the biases decrease as σ_0 decreases. Therefore, the MTSI estimates provide asymptotically unbiased estimators of the frequencies. It can be seen from Tables 1-4 that the SEs of all the parameters decrease gradually and approach the ASEs, as well as from Table 5-6 that the COVs of the corresponding frequencies decrease gradually and approach the ACOVs as the sample size increases, which verifies the consistency of the MTSI estimates. It is also observed from Tables 1-4 that the MTSI estimates are also fairly good even for small sample size and high level

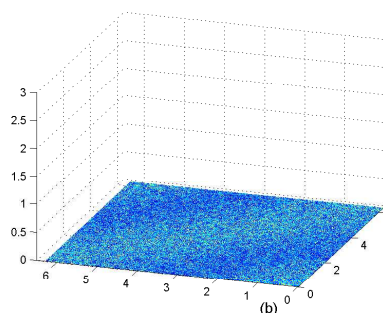


Figure 2: Plot of the 2-D periodogram function of the original observations for model (11) when (b) $M=N=256$ with $\sigma_0=1.5$

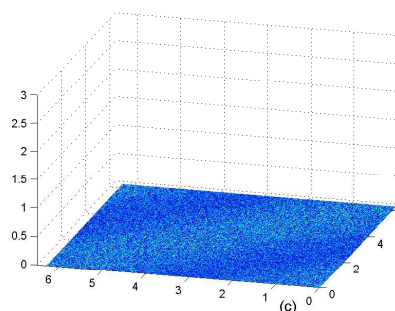


Figure 3: Plot of the 2-D periodogram function of the original observations for model (11) when (c) $M=N=512$ with $\sigma_0=1.5$

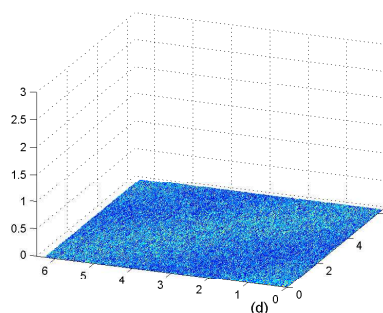


Figure 4: Plot of the 2-D periodogram function of the original observations for model (11) when (d) $M=512, N=128$ with $\sigma_0=1.5$

of noise while the initial estimates are bad, which verifies the robustness and efficiency of the MTSI algorithm.

Comparing Table 4 with Table 1 and Table 3, it is observed that the SEs for all the frequencies in Table 4 are lower than those corresponding in Table 1 and higher than those corresponding in Table 3. It is not surprising because the sample size M in Table 4 is larger than that in Table 1 while the sample size N in Table 4 is smaller than

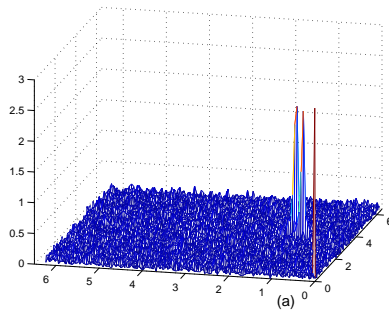


Figure 5: Plot of the 2-D periodogram function of the squared observations for model (11) when (a) $M=N=128$ with $\sigma_0=1.5$

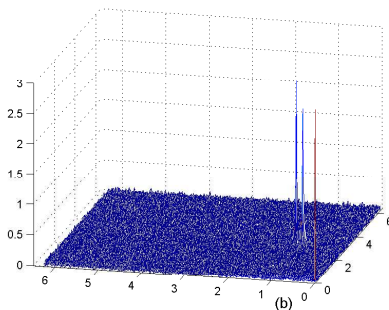


Figure 6: Plot of the 2-D periodogram function of the squared observations for model (11) when (b) $M=N=256$ with $\sigma_0=1.5$

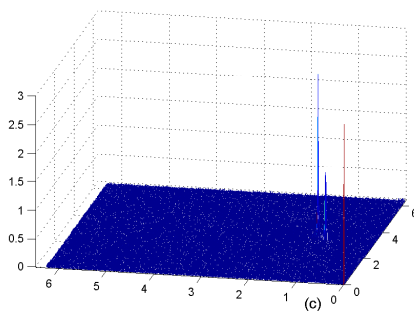


Figure 7: Plot of the 2-D periodogram function of the squared observations for model (11) when (c) $M=N=512$ with $\sigma_0=1.5$

that in Table 3. So the effectiveness of the MTSI algorithm is also verified when the sample size is not equal in the two dimensions.

5. Conclusions

In this paper, we considered the estimation of the frequencies of 2-D superimposed exponential model in

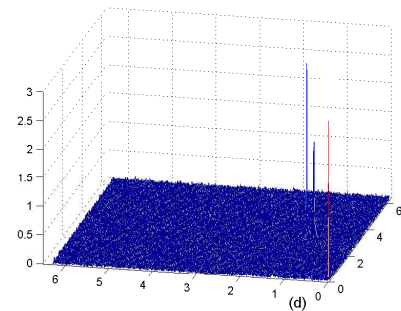


Figure 8: Plot of the 2-D periodogram function of the squared observations for model (11) when (d) $M=512$, $N=128$ with $\sigma_0=1.5$

Table 4: The average estimates of the Initial and MTSI estimator based on 100 replications, as well as the corresponding SEs and ASEs of the two frequency pairs when $M=512$ and $N=128$

σ_0	ESTI	Fr11	Fr12	Fr21	Fr22
0.5	PARA	0.50000	1.50000	0.60000	1.60000
	INIT	0.49703	1.49711	0.60132	1.59533
	MTSI	0.50000	1.50001	0.59999	1.60000
	SE	2.746e-5	1.155e-4	2.010e-5	7.885e-5
	ASE	2.724e-5	1.089e-4	1.944e-5	7.778e-5
1	PARA	0.50000	1.50000	0.60000	1.60000
	INIT	0.49713	1.49716	0.60132	1.59534
	MTSI	0.49999	1.50003	0.59999	1.59997
	SE	3.731e-5	1.369e-4	2.461e-5	9.982e-5
	ASE	3.400e-5	1.360e-4	2.470e-5	9.883e-5
1.5	PARA	0.50000	1.50000	0.60000	1.60000
	INIT	0.49715	1.49713	0.60132	1.59534
	MTSI	0.50000	1.49999	0.59999	1.59998
	SE	4.721e-5	1.792e-4	3.136e-5	1.346e-4
	ASE	4.379e-5	1.751e-4	3.238e-5	1.295e-4

Table 5: The COVs and ACOVs of Fr11 and Fr21 based on 100 replications

σ_0	EST	128,128	256,256	512,512	512,128
0.5	COV	-1.35e-8	-1.21e-9	-5.11e-11	-1.04e-9
	ACOV	-1.31e-8	-8.23e-10	-5.14e-11	-8.23e-10
	COV	-1.65e-8	-1.27e-9	-6.26e-11	-2.26e-9
1	ACOV	-1.31e-8	-8.23e-10	-5.14e-11	-8.23e-10
	COV	-2.60e-8	-1.47e-9	-8.96e-11	-2.32e-9
1.5	ACOV	-1.31e-8	-8.23e-10	-5.14e-11	-8.23e-10

presence of stationary multiplicative and additive noise. We used a two-stage joint algorithm to estimate the frequencies of the model we considered. At the first stage, a periodogram based initial estimator was given for a rough estimation. Then the MTSI algorithm was proposed to refine the initial estimator by three iterations. We proved the consistency of the MTSI estimators and obtained the asymptotic distribution of the MTSI

Table 6: The COVs and ACOVs of Fr12 and Fr22 based on 100 replications

σ_0	EST	128,128	256,256	512,512	512,128
0.5	COV	-1.32e-8	-1.14e-9	-5.39e-11	-3.23e-9
	ACOV	-1.31e-8	-8.23e-10	-5.14e-11	-8.23e-10
1	COV	-1.62e-8	-1.17e-9	-6.12e-11	-4.67e-9
	ACOV	-1.31e-8	-8.23e-10	-5.14e-11	-8.23e-10
1.5	COV	-2.64e-8	-1.82e-9	-7.41e-11	-6.42e-9
	ACOV	-1.31e-8	-8.23e-10	-5.14e-11	-8.23e-10

estimators. It is observed that the MTSI algorithm works quite well in terms of biases and mean squared errors even when the two frequency pairs are very close, and the estimators have the same convergence rate with LSE in additive noise. Since the random field model consisting of evanescent and purely indeterministic component can be seen as a special case of our model (1), we generalized the MTSI algorithm to a wider and more practical noise distribution and provide an accurate and computationally efficient algorithm for the parameter estimation of stationary random field consisting of evanescent and purely indeterministic component. Moreover, it needs only three steps to converge from the given starting value, so it naturally saves computational time and can be used for online implementation. Finally, the amplitude of the model in this paper is described to be zero mean MA process which is stationary, however, the evanescent component of a conditional random field may be non-stationary. The MTSI algorithm for this condition will be investigated later.

Acknowledgement

This work is partially supported by NSFC under Grants 61071188, 61302138, 11126274 and 61102103, by NSFC of Hubei Province under Grants 2011CDB333 and by the Fundamental Research Funds for National University, China University of Geosciences (Wuhan) under Grants CUGL100239, CUGL100236 and CCNU10A01013.

Appendix

We need to compute $\mathbf{A}_{M,N}$, $\mathbf{B}_{M,N}$ and $\mathbf{C}_{M,N}$ for the derivation of the algorithm. Firstly, we will compute $\mathbf{C}_{M,N}$. Since $\{\varepsilon_k(m,n)\}$ is an array of i.i.d. random variable with mean zero and variance σ_k^2 respectively, if we note $\eta_k(m,n) \triangleq \varepsilon_k^2(m,n) - \sigma_k^2$, then $\eta_k(m,n)$ is an array of i.i.d. variable with mean zero and variance

$$E(\varepsilon_k^4) - \sigma_k^4.$$

$$\begin{aligned}
 1/\mathbf{C}_{M,N}(j) &= \sum_{k=1}^p \sum_{m=1}^M \sum_{n=1}^N \beta_k^2(m,n) \\
 &\quad \times e^{2i[(u_k - \bar{u}_j)m + (v_k - \bar{v}_j)n + \phi_k]} \\
 &+ \sum_{m=1}^M \sum_{n=1}^N \gamma^2(m,n) e^{-2i(\bar{u}_j m + \bar{v}_j n)} \\
 &+ 2 \sum_{k=1}^p \sum_{m=1}^M \sum_{n=1}^N \beta_k(m,n) \gamma(m,n) \\
 &\quad \times e^{i[(u_k - 2\bar{u}_j)m + (v_k - 2\bar{v}_j)n + \phi_k]} \\
 &+ 2 \sum_{k=1}^p \sum_{l < k}^M \sum_{m=1}^M \sum_{n=1}^N \beta_k(m,n) \beta_l(m,n) \\
 &\quad \times e^{i[(u_k + u_l - 2u_j)m + (v_k + v_l - 2v_j)n + \phi_k + \phi_l]} \\
 &= C_1 + C_2 + C_3 + C_4, \text{ (say)} \tag{12}
 \end{aligned}$$

where

$$\begin{aligned}
 C_1 &= \sum_{k=1}^p \sum_{s=-\infty}^{+\infty} \sum_{l=-\infty}^{+\infty} a_k^2(s,l) \sigma_k^2 e^{2i\phi_k} \\
 &\quad \times \sum_{m=1}^M \sum_{n=1}^N e^{2i[(u_k - \bar{u}_j)m + (v_k - \bar{v}_j)n]} \\
 &+ \sum_{k=1}^p \sum_{m=1}^M \sum_{n=1}^N \sum_{s=-\infty}^{+\infty} \sum_{l=-\infty}^{+\infty} a_k^2(s,l) \eta_k(m-s, n-l) \\
 &\quad \times e^{2i[(u_k - \bar{u}_j)m + (v_k - \bar{v}_j)n + \phi_k]} \\
 &+ 2 \sum_{k=1}^p \sum_{m=1}^M \sum_{n=1}^N \sum_{s=-\infty}^{+\infty} \sum_{l=-\infty}^{+\infty} \sum_{s' \neq s} \sum_{l'=-\infty}^{+\infty} a_k(s,l) a_k(s',l') \\
 &\quad \times \varepsilon_k(m-s, n-l) \varepsilon_k(m-s', n-l') e^{2i[(u_k - \bar{u}_j)m + (v_k - \bar{v}_j)n + \phi_k]} \\
 &+ 2 \sum_{k=1}^p \sum_{m=1}^M \sum_{n=1}^N \sum_{s=-\infty}^{+\infty} \sum_{l=-\infty}^{+\infty} \sum_{l' \neq l} a_k(s,l) a_k(s,l') \varepsilon_k(m-s, n-l) \\
 &\quad \times \varepsilon_k(m-s, n-l') e^{2i[(u_k - \bar{u}_j)m + (v_k - \bar{v}_j)n + \phi_k]} \\
 &= \sum_{k=1}^p \sum_{s=-\infty}^{+\infty} \sum_{l=-\infty}^{+\infty} a_k^2(s,l) \sigma_k^2 e^{2i\phi_k} J_{1k}(M,N) + R_1(M,N). \text{ (say)} \tag{13}
 \end{aligned}$$

For $k \neq j$, $J_{1k}(M,N) = O_p(1)$. For $k = j$, using Taylor series approximation of $e^{2i(u_j - \bar{u}_j)m}$ and $e^{2i(v_j - \bar{v}_j)n}$ both up to first order, we have

$$\begin{aligned}
 J_{1j}(M,N) &= \sum_{m=1}^M \sum_{n=1}^N e^{2i[(u_j - \bar{u}_j)m + (v_j - \bar{v}_j)n]} \\
 &= \sum_{m=1}^M e^{2i(u_j - \bar{u}_j)m} \sum_{n=1}^N e^{2i(v_j - \bar{v}_j)n}
 \end{aligned}$$

$$\begin{aligned}
 &= \left[M + 2i(u_j - \tilde{u}_j) \sum_{m=1}^M m e^{i\theta_1(u_j - \tilde{u}_j)m} \right] \\
 &\quad \left[N + 2i(v_j - \tilde{v}_j) \sum_{n=1}^N n e^{2i\theta_2(v_j - \tilde{v}_j)n} \right] \\
 &= MN \left[1 + O_p(M^{-\delta}) + O_p(N^{-\delta}) \right], \tag{14}
 \end{aligned}$$

here $0 < \theta_1 < 1, 0 < \theta_2 < 1$. Using the independence of $\{\eta_k(m, n)\}$ and $\{\varepsilon_0(m, n)\}$, (2)-(4) and Lemma 2 of [23], we have

$$R_1(M, N) = O_p(M^{\frac{1}{2}}N^{\frac{1}{2}}), \tag{15}$$

and

$$\begin{aligned}
 C_2 &= \sum_{m=1}^M \sum_{n=1}^N \gamma^2(m, n) e^{-2i(\tilde{u}_j m + \tilde{v}_j n)} \\
 &= \sum_{s=-\infty}^{+\infty} \sum_{l=-\infty}^{+\infty} a_0^2(s, l) \sigma_0^2 \sum_{m=1}^M \sum_{n=1}^N e^{-2i(\tilde{u}_j m + \tilde{v}_j n)} \\
 &\quad + \sum_{s=-\infty}^{+\infty} \sum_{l=-\infty}^{+\infty} \sum_{m=1}^M \sum_{n=1}^N a_0^2(s, l) \eta_0(m-s, n-l) \\
 &\quad \times e^{-2i(\tilde{u}_j m + \tilde{v}_j n)} \\
 &\quad + 2 \sum_{s=-\infty}^{+\infty} \sum_{l=-\infty}^{+\infty} \sum_{s' \neq s} \sum_{l'=-\infty}^{+\infty} \sum_{m=1}^M \sum_{n=1}^N a_0(s, l) a_0(s', l') \\
 &\quad \times \varepsilon_0(m-s, n-l) \varepsilon_0(m-s', n-l') e^{-2i(\tilde{u}_j m + \tilde{v}_j n)} \\
 &\quad + 2 \sum_{s=-\infty}^{+\infty} \sum_{l=-\infty}^{+\infty} \sum_{l' \neq l} \sum_{m=1}^M \sum_{n=1}^N a_0(s, l) a_0(s, l') \\
 &\quad \times \varepsilon_0(m-s, n-l) \varepsilon_0(m-s, n-l') e^{-2i(\tilde{u}_j m + \tilde{v}_j n)} \\
 &= O_p(M^{\frac{1}{2}}N^{\frac{1}{2}}). \tag{16}
 \end{aligned}$$

Similarly, we have

$$C_3 = O_p(M^{\frac{1}{2}}N^{\frac{1}{2}}), \quad C_4 = O_p(M^{\frac{1}{2}}N^{\frac{1}{2}}). \tag{17}$$

From (12)-(17), it is immediate that

$$\begin{aligned}
 C_{M,N}(j) &= 1 \left/ \left\{ \sum_{s=-\infty}^{+\infty} \sum_{l=-\infty}^{+\infty} a_j^2(s, l) \sigma_j^2 e^{2i\phi_j} MN \right. \right. \\
 &\quad \left. \left. \left[1 + O_p(M^{-\delta}) + O_p(N^{-\delta}) \right] \right\} \right. \tag{18}
 \end{aligned}$$

Secondly, we will compute $\mathbf{A}_{M,N}$ in the following:

$$\begin{aligned}
 \mathbf{A}_{M,N}(j) &= \sum_{k=1}^p \sum_{m=1}^M \sum_{n=1}^N \beta_k^2(m, n) \left(m - \frac{M}{2}\right) \\
 &\quad \times e^{2i[(u_k - \tilde{u}_j)m + (v_k - \tilde{v}_j)n + \phi_k]} \\
 &\quad + \sum_{m=1}^M \sum_{n=1}^N \gamma^2(m, n) \left(m - \frac{M}{2}\right) e^{-2i(\tilde{u}_j m + \tilde{v}_j n)} \\
 &\quad + 2 \sum_{k=1}^p \sum_{m=1}^M \sum_{n=1}^N \left(m - \frac{M}{2}\right) \beta_k(m, n) \gamma(m, n) \\
 &\quad \times e^{i[(u_k - 2\tilde{u}_j)m + (v_k - 2\tilde{v}_j)n + \phi_k]} \\
 &\quad + 2 \sum_{k=1}^p \sum_{l < k} \sum_{m=1}^M \sum_{n=1}^N \beta_k(m, n) \beta_l(m, n) \left(m - \frac{M}{2}\right) \\
 &\quad \times e^{i[(u_k + u_l - 2\tilde{u}_j)m + (v_k + v_l - 2\tilde{v}_j)n + \phi_k + \phi_l]} \\
 &= A_1 + A_2 + A_3 + A_4, \text{ (say)} \tag{19}
 \end{aligned}$$

where

$$\begin{aligned}
 A_1 &= \sum_{k=1}^p \sum_{s=-\infty}^{+\infty} \sum_{l=-\infty}^{+\infty} a_k^2(s, l) \sigma_k^2 e^{2i\phi_k} \sum_{m=1}^M \sum_{n=1}^N \left(m - \frac{M}{2}\right) \\
 &\quad \times e^{2i[(u_k - \tilde{u}_j)m + (v_k - \tilde{v}_j)n]} \\
 &\quad + \sum_{k=1}^p \sum_{m=1}^M \sum_{n=1}^N \sum_{s=-\infty}^{+\infty} \sum_{l=-\infty}^{+\infty} a_k^2(s, l) \eta_k(m-s, n-l) \\
 &\quad \times \left(m - \frac{M}{2}\right) e^{2i[(u_k - \tilde{u}_j)m + (v_k - \tilde{v}_j)n + \phi_k]} \\
 &\quad + 2 \sum_{k=1}^p \sum_{m=1}^M \sum_{n=1}^N \sum_{s=-\infty}^{+\infty} \sum_{l=-\infty}^{+\infty} \sum_{s' \neq s} \sum_{l'=-\infty}^{+\infty} a_k(s, l) a_k(s', l') \\
 &\quad \times \varepsilon_k(m-s, n-l) \varepsilon_k(m-s', n-l') \left(m - \frac{M}{2}\right) \\
 &\quad \times e^{2i[(u_k - \tilde{u}_j)m + (v_k - \tilde{v}_j)n + \phi_k]} \\
 &\quad + 2 \sum_{k=1}^p \sum_{m=1}^M \sum_{n=1}^N \sum_{s=-\infty}^{+\infty} \sum_{l=-\infty}^{+\infty} \sum_{l' \neq l} a_k(s, l) a_k(s, l') \\
 &\quad \times \varepsilon_k(m-s, n-l) \varepsilon_k(m-s, n-l') \left(m - \frac{M}{2}\right) \\
 &\quad \times e^{2i[(u_k - \tilde{u}_j)m + (v_k - \tilde{v}_j)n + \phi_k]} \\
 &= \sum_{k=1}^p \sum_{s=-\infty}^{+\infty} \sum_{l=-\infty}^{+\infty} a_k^2(s, l) \sigma_k^2 e^{2i\phi_k} J_{2k}(M, N) + R_2(M, N). \tag{20}
 \end{aligned}$$

For $k \neq j$, $J_{2k}(M, N) = O_p(M)$. For $k = j$, using Taylor series approximation of $e^{2i(u_j - \tilde{u}_j)m}$ and $e^{2i(v_j - \tilde{v}_j)n}$ both up to first order, we have

$$\begin{aligned}
 J_{2j}(M, N) &= \\
 &\quad \left[\sum_{m=1}^M \left(m - \frac{M}{2}\right) + i(u_j - \tilde{u}_j) \frac{M(M+1)(M+2)}{6} \right. \\
 &\quad \left. - 2(u_j - \tilde{u}_j)^2 \sum_{m=1}^M \left(m - \frac{M}{2}\right) m^2 e^{2i\theta_3(u_j - \tilde{u}_j)m} \right]
 \end{aligned}$$

$$\begin{aligned} & \times \left[N + 2i(v_j - \tilde{v}_j) \sum_{n=1}^N ne^{2i\theta_4(v_j - \tilde{v}_j)n} \right] \\ & = i(u_j - \tilde{u}_j) \frac{M^3 N}{6} \left[1 + O_p(M^{-\delta}) + O_p(N^{-\delta}) \right], \end{aligned} \tag{21}$$

here $0 < \theta_3 < 1, 0 < \theta_4 < 1$. Using Taylor series approximation of $e^{i[(u_j - \tilde{u}_j)m + (v_j - \tilde{v}_j)n]}$ up to first order and Lemma 2 of [23], we have

$$\begin{aligned} R_2(M, N) &= \sum_{k=1}^p \sum_{m=1}^M \sum_{n=1}^N \sum_{s=-\infty}^{+\infty} \sum_{l=-\infty}^{+\infty} a_k^2(s, l) \\ & \times \eta_k(m - s, n - l) \left(m - \frac{M}{2}\right) e^{2i[(u_k - u_j)m + (v_k - v_j)n + \phi_k]} \\ & + 2 \sum_{k=1}^p \sum_{m=1}^M \sum_{n=1}^N \sum_{s=-\infty}^{+\infty} \sum_{l=-\infty}^{+\infty} \sum_{s' \neq s} \sum_{l'=-\infty}^{+\infty} a_k(s, l) a_k(s', l') \\ & \times \left(m - \frac{M}{2}\right) \varepsilon_k(m - s, n - l) \varepsilon_k(m - s', n - l') \\ & \times e^{2i[(u_k - u_j)m + (v_k - v_j)n + \phi_k]} \\ & + 2 \sum_{k=1}^p \sum_{m=1}^M \sum_{n=1}^N \sum_{s=-\infty}^{+\infty} \sum_{l=-\infty}^{+\infty} \sum_{l' \neq l} a_k(s, l) a_k(s, l') \\ & \times \left(m - \frac{M}{2}\right) \varepsilon_k(m - s, n - l) \varepsilon_k(m - s, n - l') \\ & \times e^{2i[(u_k - u_j)m + (v_k - v_j)n + \phi_k]} \\ & + O_p(M^{\frac{3}{2} - \delta} N^{\frac{1}{2}}) + O_p(M^{\frac{3}{2}} N^{\frac{1}{2} - \delta}). \end{aligned} \tag{22}$$

Similarly, we have

$$\begin{aligned} A_2 &= \sum_{m=1}^M \sum_{n=1}^N \gamma^2(m, n) \left(m - \frac{M}{2}\right) e^{-2i(\tilde{u}_j m + \tilde{v}_j n)} \\ & = \sum_{s=-\infty}^{+\infty} \sum_{l=-\infty}^{+\infty} a_0^2(s, l) \sigma_0^2 \sum_{m=1}^M \sum_{n=1}^N \left(m - \frac{M}{2}\right) e^{-2i(u_j m + v_j n)} \\ & + \sum_{m=1}^M \sum_{n=1}^N \sum_{s=-\infty}^{+\infty} \sum_{l=-\infty}^{+\infty} a_0^2(s, l) \eta_0(m - s, n - l) \left(m - \frac{M}{2}\right) \\ & \times e^{-2i(u_j m + v_j n)} \\ & + 2 \sum_{m=1}^M \sum_{n=1}^N \sum_{s=-\infty}^{+\infty} \sum_{l=-\infty}^{+\infty} \sum_{s' \neq s} \sum_{l'=-\infty}^{+\infty} a_0(s, l) a_0(s', l') \\ & \times \varepsilon_0(m - s, n - l) \varepsilon_0(m - s', n - l') \left(m - \frac{M}{2}\right) \\ & \times e^{-2i(u_j m + v_j n)} \\ & + 2 \sum_{m=1}^M \sum_{n=1}^N \sum_{s=-\infty}^{+\infty} \sum_{l=-\infty}^{+\infty} \sum_{l' \neq l} a_0(s, l) a_0(s, l') \\ & \times \varepsilon_0(m - s, n - l) \varepsilon_0(m - s, n - l') \left(m - \frac{M}{2}\right) \\ & \times e^{-2i(u_j m + v_j n)} \\ & + O_p(M^{\frac{3}{2} - \delta} N^{\frac{1}{2}}) + O_p(M^{\frac{3}{2}} N^{\frac{1}{2} - \delta}), \end{aligned} \tag{23}$$

$$\begin{aligned} A_3 &= 2 \sum_{k=1}^p \sum_{m=1}^M \sum_{n=1}^N \beta_k(m, n) \gamma(m, n) \left(m - \frac{M}{2}\right) \\ & \times e^{i[(u_k - 2\tilde{u}_j)m + (v_k - 2\tilde{v}_j)n + \phi_k]} \\ & = 2 \sum_{k=1}^p \sum_{m=1}^M \sum_{n=1}^N \sum_{s=-\infty}^{+\infty} \sum_{l=-\infty}^{+\infty} \sum_{s'=-\infty}^{+\infty} \sum_{l'=-\infty}^{+\infty} a_k(s, l) a_0(s', l') \\ & \times \varepsilon_k(m - s, n - l) \varepsilon_0(m - s', n - l') \left(m - \frac{M}{2}\right) \\ & \times e^{i[(u_k - 2u_j)m + (v_k - 2v_j)n + \phi_k]} \\ & + O_p(M^{\frac{3}{2} - \delta} N^{\frac{1}{2}}) + O_p(M^{\frac{3}{2}} N^{\frac{1}{2} - \delta}), \end{aligned} \tag{24}$$

and

$$\begin{aligned} A_4 &= 2 \sum_{k=1}^p \sum_{l < k} \sum_{m=1}^M \sum_{n=1}^N \beta_k(m, n) \beta_l(m, n) \left(m - \frac{M}{2}\right) \\ & \times e^{i[(u_k + u_l - 2\tilde{u}_j)m + (v_k + v_l - 2\tilde{v}_j)n + \phi_k + \phi_l]} \\ & = 2 \sum_{k=1}^p \sum_{l < k} \sum_{m=1}^M \sum_{n=1}^N \sum_{s=-\infty}^{+\infty} \sum_{t=-\infty}^{+\infty} \sum_{s'=-\infty}^{+\infty} \sum_{t'=-\infty}^{+\infty} a_k(s, t) \\ & \times a_l(s', t') \left(m - \frac{M}{2}\right) \varepsilon_k(m - s, n - t) \varepsilon_l(m - s', n - t') \\ & \times e^{i[(u_k + u_l - 2\tilde{u}_j)m + (v_k + v_l - 2\tilde{v}_j)n + \phi_k + \phi_l]} \\ & + O_p(M^{\frac{3}{2} - \delta} N^{\frac{1}{2}}) + O_p(M^{\frac{3}{2}} N^{\frac{1}{2} - \delta}). \end{aligned} \tag{25}$$

From (19)-(25), it is immediate that

$$\begin{aligned} \mathbf{A}_{M, N}(j) &= i \sum_{s=-\infty}^{+\infty} \sum_{l=-\infty}^{+\infty} a_j^2(s, l) \sigma_j^2 e^{2i\phi_j} (u_j - \tilde{u}_j) \frac{M^3 N}{6} \\ & \times \left[1 + O_p(M^{-\delta}) + O_p(N^{-\delta}) \right] \\ & + \sum_{k=1}^p \sum_{m=1}^M \sum_{n=1}^N \sum_{s=-\infty}^{+\infty} \sum_{l=-\infty}^{+\infty} a_k^2(s, l) \eta_k(m - s, n - l) \left(m - \frac{M}{2}\right) \\ & \times e^{2i[(u_k - u_j)m + (v_k - v_j)n + \phi_k]} \\ & + 2 \sum_{k=1}^p \sum_{m=1}^M \sum_{n=1}^N \sum_{s=-\infty}^{+\infty} \sum_{l=-\infty}^{+\infty} \sum_{s' \neq s} \sum_{l'=-\infty}^{+\infty} a_k(s, l) a_k(s', l') \\ & \times \varepsilon_k(m - s, n - l) \varepsilon_k(m - s', n - l') \left(m - \frac{M}{2}\right) \\ & \times e^{2i[(u_k - u_j)m + (v_k - v_j)n + \phi_k]} \\ & + 2 \sum_{k=1}^p \sum_{m=1}^M \sum_{n=1}^N \sum_{s=-\infty}^{+\infty} \sum_{l=-\infty}^{+\infty} \sum_{l' \neq l} a_k(s, l) a_k(s, l') \varepsilon_k(m - s, n - l) \\ & \times \varepsilon_k(m - s, n - l') \left(m - \frac{M}{2}\right) e^{2i[(u_k - u_j)m + (v_k - v_j)n + \phi_k]} \\ & + \sum_{m=1}^M \sum_{n=1}^N \sum_{s=-\infty}^{+\infty} \sum_{l=-\infty}^{+\infty} a_0^2(s, l) \eta_0(m - s, n - l) \left(m - \frac{M}{2}\right) \\ & \times e^{-2i(u_j m + v_j n)} \\ & + 2 \sum_{m=1}^M \sum_{n=1}^N \sum_{s=-\infty}^{+\infty} \sum_{l=-\infty}^{+\infty} \sum_{s' \neq s} \sum_{l'=-\infty}^{+\infty} a_0(s, l) a_0(s', l') \\ & \times \varepsilon_0(m - s, n - l) \varepsilon_0(m - s', n - l') \left(m - \frac{M}{2}\right) e^{-2i(u_j m + v_j n)} \end{aligned}$$

$$\begin{aligned}
 &+2 \sum_{m=1}^M \sum_{n=1}^N \sum_{s=-\infty}^{+\infty} \sum_{l=-\infty}^{+\infty} \sum_{l' \neq l} a_0(s, l) a_0(s, l') \\
 &\times \varepsilon_0(m-s, n-l) \varepsilon_0(m-s, n-l') \left(m - \frac{M}{2}\right) e^{-2i(u_j m + v_j n)} \\
 &+2 \sum_{k=1}^p \sum_{m=1}^M \sum_{n=1}^N \sum_{s=-\infty}^{+\infty} \sum_{l=-\infty}^{+\infty} \sum_{s'=-\infty}^{+\infty} \sum_{l'=-\infty}^{+\infty} a_k(s, l) a_0(s', l') \\
 &\times \varepsilon_k(m-s, n-l) \varepsilon_0(m-s', n-l') \left(m - \frac{M}{2}\right) \\
 &\times e^{i[(u_k - 2u_j)m + (v_k - 2v_j)n + \phi_k]} \\
 &+2 \sum_{k=1}^p \sum_{l < k} \sum_{m=1}^M \sum_{n=1}^N \sum_{s=-\infty}^{+\infty} \sum_{t=-\infty}^{+\infty} \sum_{s'=-\infty}^{+\infty} \sum_{t'=-\infty}^{+\infty} a_k(s, t) \\
 &\times a_l(s', t') \varepsilon_k(m-s, n-t) \varepsilon_l(m-s', n-t') \left(m - \frac{M}{2}\right) \\
 &\times e^{i[(u_k - 2u_j)m + (v_k - 2v_j)n + \phi_k]} \\
 &+O_p(M^{\frac{3}{2}-\delta} N^{\frac{1}{2}}) + O_p(M^{\frac{3}{2}} N^{\frac{1}{2}-\delta}). \tag{26}
 \end{aligned}$$

Therefore

$$\begin{aligned}
 \hat{\mathbf{u}} &= \tilde{\mathbf{u}} + \frac{6}{M^2} \text{Im}[\mathbf{A}_{M,N} \odot \mathbf{C}_{M,N}] \\
 &= \mathbf{u} + (\mathbf{u} - \tilde{\mathbf{u}}) \left[O_p(M^{-\delta}) + O_p(N^{-\delta}) \right] \\
 &\quad + \frac{6}{M^3 N} \mathbf{X}, \text{ (say)}
 \end{aligned}$$

where

$$\begin{aligned}
 \mathbf{X}(j) &\triangleq \left\{ \sum_{k=1}^p \sum_{m=1}^M \sum_{n=1}^N \sum_{s=-\infty}^{+\infty} \sum_{l=-\infty}^{+\infty} a_k^2(s, l) \right. \\
 &\quad \times \eta_k(m-s, n-l) \left(m - \frac{M}{2}\right) \\
 &\quad \times \sin 2[(u_k - u_j)m + (v_k - v_j)n + \phi_k - \phi_j] \\
 &+2 \sum_{k=1}^p \sum_{m=1}^M \sum_{n=1}^N \sum_{s=-\infty}^{+\infty} \sum_{l=-\infty}^{+\infty} \sum_{s' \neq s} \sum_{l'=-\infty}^{+\infty} a_k(s, l) a_k(s', l') \\
 &\quad \times \varepsilon_k(m-s, n-l) \varepsilon_k(m-s', n-l') \left(m - \frac{M}{2}\right) \\
 &\quad \times \sin 2[(u_k - u_j)m + (v_k - v_j)n + \phi_k - \phi_j] \\
 &+2 \sum_{k=1}^p \sum_{m=1}^M \sum_{n=1}^N \sum_{s=-\infty}^{+\infty} \sum_{l=-\infty}^{+\infty} \sum_{l' \neq l} a_k(s, l) a_k(s, l') \\
 &\quad \times \varepsilon_k(m-s, n-l) \varepsilon_k(m-s, n-l') \left(m - \frac{M}{2}\right) \\
 &\quad \times \sin 2[(u_k - u_j)m + (v_k - v_j)n + \phi_k - \phi_j] \\
 &- \sum_{m=1}^M \sum_{n=1}^N \sum_{s=-\infty}^{+\infty} \sum_{l=-\infty}^{+\infty} a_0^2(s, l) \eta_0(m-s, n-l) \\
 &\quad \times \varepsilon_0(m-s, n-l) \left(m - \frac{M}{2}\right) \sin 2(u_j m + v_j n + \phi_j) \\
 &-2 \sum_{m=1}^M \sum_{n=1}^N \sum_{s=-\infty}^{+\infty} \sum_{l=-\infty}^{+\infty} \sum_{s' \neq s} \sum_{l'=-\infty}^{+\infty} a_0(s, l) a_0(s', l')
 \end{aligned}$$

$$\begin{aligned}
 &\times \varepsilon_0(m-s', n-l') \left(m - \frac{M}{2}\right) \sin 2i(u_j m + v_j n + \phi_j) \\
 &-2 \sum_{m=1}^M \sum_{n=1}^N \sum_{s=-\infty}^{+\infty} \sum_{l=-\infty}^{+\infty} \sum_{l' \neq l} a_0(s, l) a_0(s', l') \\
 &\times \varepsilon_0(m-s, n-l) \varepsilon_0(m-s, n-l') \left(m - \frac{M}{2}\right) \\
 &\times \sin 2i(u_j m + v_j n + \phi_j) \\
 &+2 \sum_{k=1}^p \sum_{m=1}^M \sum_{n=1}^N \sum_{s=-\infty}^{+\infty} \sum_{l=-\infty}^{+\infty} \sum_{s'=-\infty}^{+\infty} \sum_{l'=-\infty}^{+\infty} a_k(s, l) a_0(s', l') \\
 &\times \varepsilon_k(m-s, n-l) \varepsilon_0(m-s', n-l') \left(m - \frac{M}{2}\right) \\
 &\times \sin [(u_k - 2u_j)m + (v_k - 2v_j)n + \phi_k - 2\phi_j] \\
 &+2 \sum_{k=1}^p \sum_{l=1}^p \sum_{m=1}^M \sum_{n=1}^N \sum_{s=-\infty}^{+\infty} \sum_{t=-\infty}^{+\infty} \sum_{s'=-\infty}^{+\infty} \sum_{t'=-\infty}^{+\infty} a_k(s, t) \\
 &\times a_l(s', t') \varepsilon_k(m-s, n-t) \varepsilon_l(m-s', n-t') \left(m - \frac{M}{2}\right) \\
 &\times \sin [(u_k - 2u_j)m + (v_k - 2v_j)n + \phi_k - 2\phi_j] \Big\} \\
 &\quad \Big/ \sum_{s=-\infty}^{+\infty} \sum_{l=-\infty}^{+\infty} a_j^2(s, l) \sigma_j^2.
 \end{aligned}$$

Similarly, we have

$$\begin{aligned}
 \hat{\mathbf{v}} &= \tilde{\mathbf{v}} + \frac{6}{N^2} \text{Im}[\mathbf{B}_{M,N} \odot \mathbf{C}_{M,N}] \\
 &= \mathbf{v} + (\mathbf{v} - \tilde{\mathbf{v}}) \left[O_p(M^{-\delta}) + O_p(N^{-\delta}) \right] \\
 &\quad + \frac{6}{N^3 M} \mathbf{Y}, \text{ (say)} \tag{28}
 \end{aligned}$$

where \mathbf{Y} is similar with \mathbf{X} and can be obtained by substituting $(m - \frac{M}{2})$ in each term of \mathbf{X} with $(n - \frac{N}{2})$. Using Lemmas 1 and Lemma 2 of [23], we have when $\min\{M, N\} \rightarrow \infty$

$$\begin{aligned}
 \text{var} \left[\frac{6}{M^{\frac{3}{2}} N^{\frac{1}{2}}} \mathbf{X}(j) \right] &\rightarrow (\Sigma_1)_{jj}, \\
 \text{var} \left[\frac{6}{M^{\frac{1}{2}} N^{\frac{3}{2}}} \mathbf{Y}(j) \right] &\rightarrow (\Sigma_2)_{jj}, \\
 \text{Cov} \left[\frac{6}{M^{\frac{3}{2}} N^{\frac{1}{2}}} \mathbf{X}(j), \frac{6}{M^{\frac{1}{2}} N^{\frac{3}{2}}} \mathbf{Y}(j) \right] &\rightarrow 0, \tag{29}
 \end{aligned}$$

where $(\Sigma_1)_{jj}$ and $(\Sigma_2)_{jj}$ are defined in Theorem 1. For $j \neq \tau$, we have

$$\begin{aligned}
 \text{var} \left[\frac{6}{M^{\frac{3}{2}} N^{\frac{1}{2}}} \mathbf{X}(j), \frac{6}{M^{\frac{3}{2}} N^{\frac{1}{2}}} \mathbf{X}(\tau) \right] &\rightarrow (\Sigma_1)_{j\tau}, \\
 \text{var} \left[\frac{6}{M^{\frac{1}{2}} N^{\frac{3}{2}}} \mathbf{Y}(j), \frac{6}{M^{\frac{1}{2}} N^{\frac{3}{2}}} \mathbf{Y}(\tau) \right] &\rightarrow (\Sigma_2)_{j\tau}, \\
 \text{Cov} \left[\frac{6}{M^{\frac{3}{2}} N^{\frac{1}{2}}} \mathbf{X}(j), \frac{6}{M^{\frac{1}{2}} N^{\frac{3}{2}}} \mathbf{Y}(\tau) \right] &\rightarrow 0, \tag{30}
 \end{aligned}$$

where $(\Sigma_1)_{j\tau}$ and $(\Sigma_2)_{j\tau}$ are defined in Theorem 1.

From assumption (iii), we have $O_p(M^{-\frac{3}{2}}N^{-\frac{1}{2}}) = O_p(M^{-\frac{1}{2}}N^{-\frac{3}{2}}) = O_p(M^{-2}) = O_p(N^{-2})$. Therefore, if $\hat{\mathbf{u}} - \mathbf{u} = O_p(M^{-1-\delta})\mathbf{I}_p$, $\hat{\mathbf{v}} - \mathbf{v} = O_p(N^{-1-\delta})\mathbf{I}_p$ and $0 < \delta \leq \frac{1}{2}$, then from (27) and (28), $\hat{\mathbf{u}} - \mathbf{u} = O_p(M^{-1-2\delta})\mathbf{I}_p$, $\hat{\mathbf{v}} - \mathbf{v} = O_p(N^{-1-2\delta})\mathbf{I}_p$. If $\frac{1}{2} < \delta \leq 1$, from (27)-(30) and using the Central Limit Theorem of linear process [27], it follows that:

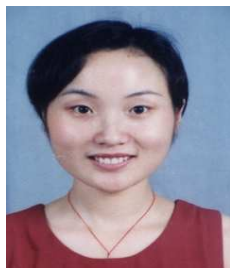
$$\left[M^{\frac{3}{2}}N^{\frac{1}{2}}(\hat{\mathbf{u}} - \mathbf{u}), M^{\frac{1}{2}}N^{\frac{3}{2}}(\hat{\mathbf{v}} - \mathbf{v}) \right] \xrightarrow{\mathcal{L}} \mathcal{N}_{2p} \left(\mathbf{0}, \begin{bmatrix} \Sigma_1 & \mathbf{0} \\ \mathbf{0} & \Sigma_2 \end{bmatrix} \right).$$

References

- [1] P. Stoica and R. Moses, *Spectral Analysis of Signals*. Prentice-Hall, NJ: Upper Saddle River, (2005).
- [2] P. Masson, W. Pieczynski, SEM algorithm and unsupervised statistical segmentation of satellite images, *Geoscience and Remote Sensing*, IEEE Transactions on, **31**, 618-633 (1993).
- [3] P. A. Burrough, Principles of geographical information systems for land resources assessment Principles of geographical information systems for land resources assessment, Geocarto International, **1**, (1986).
- [4] J S Bendat and A G Piersol, *Random Data Analysis and Measurement Procedures*, Measurement Science and Technology, **11**, (2000).
- [5] J. M. Francos, A. Narashimhan and J.W. Woods, *Maximum-likelihood parameter estimation of the harmonic, evanescent and purely indeterministic components of discrete homogeneous random fields*, IEEE Trans. Inf. Theory, **42**, 916-930 (1996).
- [6] G. Cohen and J.M. Francos, *A Least Squares estimation of 2-D sinusoids in colored noise: asymptotic analysis*, IEEE Trans. Inf. Theory, **48**, 2243-2252 (2002).
- [7] J. M. Francos, A. Narashimhan and J.W. Woods, *Maximum-likelihood estimation of textures using a wold decomposition model*, IEEE Trans. Image Process., **4**, 1655-1666 (1995).
- [8] Xuanli Lisa Xie, Beni, G., A validity measure for fuzzy clustering, *Pattern Analysis and Machine Intelligence*, IEEE Transactions on, **13**, 841-847 (1991).
- [9] D. Kundu and A. Mitra, *Asymptotic properties of the Least Squares estimators of 2-D exponential signals*, Multidimens. Syst. Signal Process, **7**, 135-150 (1996).
- [10] D. Kundu and R. D. Gupta, *Asymptotic properties of the least squares estimates of a two dimensional model*, *Metrika*, **48**, 83-97 (1998).
- [11] S. Nandi, D. Kundu and R. K. Srivastava, *Noise space decomposition method for two-dimensional sinusoidal model*, *Comput. Stat. Data Anal.*, (2011)
- [12] S. Nandi, A. Prasad and D. Kundu, *An efficient and fast algorithm for estimating the parameters of two-dimensional sinusoidal signals*, *J. Stat. Plan. Infer.*, **140**, 153-168 (2010).
- [13] S. Rouquette and M. Najim, *Estimation of frequencies and Damping factors by two-dimensional ESPRIT type method*, IEEE Trans. Signal Process, **49**, 237-245 (2001).
- [14] C. R. Rao, L. Zhao and B. Zhou, *Maximum likelihood estimation of 2-D superimposed exponential signals*, IEEE Trans. Signal Process, **42**, 1795-1802 (1994).
- [15] M. Kliger and J. M. Francos, *Strong consistency of the over and underdetermined LSE of 2-D exponentials in white noise*, IEEE Trans. Signal Process, **51**, 3314-3321 (2005).
- [16] Y. Hua, *Estimating two-dimensional frequencies by matrix enhancement and matrix pencil*, IEEE Trans. Signal Process, **40**, 2267-2280 (1992).
- [17] M. M. Barbieri and P. Barone, *A two-dimensional Prony's method for spectral estimation*, IEEE Trans. Signal Process, **40**, 2747-2756 (1992).
- [18] F. Vanpoucke, M. Moonen and Y. Berthoumieu, *An efficient subspace algorithm for 2-D harmonic retrieval*, in *Proceedings of ICASSP*, Adelaide, Australia, 461-464 (1994).
- [19] Z. D. Bai, C. R. Rao, M. Chow and D. Kundu, *An efficient algorithm for estimating the parameters of superimposed exponential signals*, *J. Stat. Plan. Infer.*, **110**, 23-34 (2003).
- [20] S. Nandi and D. Kundu, *An efficient and fast algorithm for estimating the parameters of sinusoidal signals*, *Sankhya*, **68**, 283-306 (2006).
- [21] J. Bian, H. Li and H. Peng, *An efficient and fast algorithm for estimating the frequencies of superimposed exponential signals in multiplicative and additive noise*, *J. Inf. Comput. Sci.*, 1785-1797 (2009).
- [22] J. Bian, H. Li and H. Peng, *An efficient and fast algorithm for estimating the frequencies of superimposed exponential signals in zero-mean multiplicative and additive noise*, *J. Stat. Comput. Simul.*, **74**, 1407-1423 (2009).
- [23] J. Bian, H. Li and H. Peng, *An efficient and fast algorithm for estimating the frequencies of 2-D superimposed exponential signals in zero-mean multiplicative and additive noise*, *J. Stat. Plan. Infer.*, **141**, 1277-1289 (2011).
- [24] Mallat, S.G., Zhang, Z., *Matching pursuits with time-frequency dictionaries*, *Signal Processing*, IEEE Transactions on, **41**, 3397-3415 (1993).
- [25] J. M. Francos, A. Z. Meiri and B. Porat, *A Wold-like decomposition of two-dimensional discrete homogeneous random fields*, *Ann. Appl. Probab.*, **5**, 248-260 (1995).
- [26] R. A. Horn and C. R. Johnson, *Matrix Analysis*, Cambridge University Press, Cambridge, (1985).
- [27] W. A. Fuller, *Introduction to Statistical Time Series*, 2nd ed., Wiley, New York, (1996).



Jiawen Bian received his M.Sc. degree in applied mathematics in 2004 from Hubei University and Ph.D. degree in earth exploration and information technology in 2010 from the China University of Geosciences. He is currently an associate professor at the School of Mathematics and Physics, China University of Geosciences, Wuhan. His research interests include statistical signal processing and time series analysis.



Jing Xing received the M.Sc. degree from the School of Mathematics and Statistics, Huazhong University of Sciences and Technology, Wuhan, China, in 2008. She is currently pursuing the Ph.D. degree at the Institute of Geophysics and Geomatics, China University of Geosciences, Wuhan. She is a lecturer at the Institute of Statistics, Hubei University of Economics, Wuhan. Her research interest is statistical signal processing.



Huiming Peng was born in Hunan, China. He received his M.Sc. degree in probability and statistics in 2005 from Wuhan University and Ph.D. degree in earth exploration and information technology in 2011 from the China University of Geosciences. His research interests include statistical signal processing and Bioinformatics.



Hongwei Li received the Ph.D. degree in applied mathematics from Peking University, Beijing, China, in 1996. From 1996 to 1998, he was a postdoctoral fellow at the Institute of Information Science, Beijing Jiaotong University. Since 1999, he has been a professor at the School of Mathematics and Physics, China University of Geosciences, Wuhan. His research interests include statistical signal processing, blind signal processing, multidimensional signal processing, pattern recognition and time series analysis.